



**HAL**  
open science

## Thermal stability of some glassy compositions of the Ge-As-Te ternary

Laurent Aldon, P.E. Lippens, Josette Olivier-Fourcade, Jean-Claude Jumas

► **To cite this version:**

Laurent Aldon, P.E. Lippens, Josette Olivier-Fourcade, Jean-Claude Jumas. Thermal stability of some glassy compositions of the Ge-As-Te ternary. *Chalcogenide Letters*, 2010, 7, pp.187-196. hal-00657461

**HAL Id: hal-00657461**

**<https://hal.science/hal-00657461>**

Submitted on 6 Jan 2012

**HAL** is a multi-disciplinary open access archive for the deposit and dissemination of scientific research documents, whether they are published or not. The documents may come from teaching and research institutions in France or abroad, or from public or private research centers.

L'archive ouverte pluridisciplinaire **HAL**, est destinée au dépôt et à la diffusion de documents scientifiques de niveau recherche, publiés ou non, émanant des établissements d'enseignement et de recherche français ou étrangers, des laboratoires publics ou privés.

**Thermal stability of some glassy compositions of the Ge-As-Te ternary system.**

**L. Aldon<sup>(1)</sup>, Mathurin Leh Deli<sup>(2)</sup>, P.E. Lippens<sup>(1)</sup>, J. Olivier-Fourcade<sup>(1)</sup> and J.C. Jumas<sup>(1)</sup>**

*<sup>(1)</sup>Laboratoire des Agrégats, Interfaces et Matériaux pour l'Energie,  
Institut Charles Gerhardt, UMR 5253 CNRS, Université Montpellier II,  
Place Eugène Bataillon, F-34095 Montpellier Cedex 5, France*

*<sup>(2)</sup>Laboratoire de chimie des matériaux inorganiques,*

*Université de Cocody,*

*22 Bp 582 Abidjan 22, Côte D'Ivoire*

**Abstract**

Tellurium-based chalcogenide glasses have been studied extensively in the recent past not only because of their technological applications, but also due to their interesting physical properties. Tellurium is a good element for far infrared transmission but is a poor glass former. Glass forming domains are very narrow in binary Ge-Te or As-Te system. Better glass forming ability and thermal stability are observed in presence of arsenic and germanium atoms. These glasses possess a wide optical window that is maximal for the  $\text{Ge}_{10}\text{As}_{20}\text{Te}_{70}$  glass (20 $\mu\text{m}$ ). It made it possible to show that the substitution of germanium by selenium and antimony reduces the physical properties ( $\rho$ ,  $E_g$ ,  $T_g$ ,  $T_{c1}$ ,  $T_{c2}$ ,  $T_{c1}-T_g$  et  $T_m$ ). Indeed germanium supports the formation of glasses, contrary to metal antimony.

**Keywords: chalcogenide glasses, X-ray diffraction, Thermal behavior, optical properties**

## 1. Introduction

Vitreous materials have thermo-physical and mechanical properties that make them suitable for many applications in various devices using light wave emission, transmission or detection. These device functions depend on optical and electronic characteristics, such as electrical conductivity [1,2], the gap width and its nature. Chalcogenide glasses offer a range of infrared transmitting materials that are transparent in the regions of 3-5 $\mu\text{m}$  and 8-14 $\mu\text{m}$ . Thus, observed transmitting ranges in glasses are 0.6-15 $\mu\text{m}$  for sulfides, 1-18 $\mu\text{m}$  for selenides and 2-20 $\mu\text{m}$  for tellurides. Chalcogenide glasses have also a high refractive index, low optical losses and their possible applications as infrared optical materials have been discussed [3,4]. Glasses of binaries As-Te [5] and Ge-Te [6] have been extensively studied as regards to their optical properties because they are transparent to infrared radiation from 2 to 18 $\mu\text{m}$  [7,8]. These glasses are good candidates for exoplanet atmosphere detection [9]. Other studies have been carried out on their electrical properties, density, heat capacities, and electrical properties [10,11].

The Ge-As-Te ternary system shows the existence of the quasi-binary  $n\text{GeTe-As}_2\text{Te}_3$  crystalline phases (with  $n = 1, 3, 5$ ) [12,13] separating two glass forming regions [14,15]. We have represented in **Figure 1** the main crystalline phases, and some glassy compositions under investigation in the 'Te-rich' and 'As-rich' regions. Having in mind the fact that the area of glassy state of the Ge-Te and As-Te binary systems is relatively small, and that Te-containing glasses exhibit an increased tendency towards crystallization [16], melt cooling was carried out by quenching in iced water. So, structural information on telluride glasses is needed in order to characterize the local order in these materials. Among the different experimental tools, differential scanning calorimetry and optical absorption spectroscopy provide valuable information for chalcogenide glasses. Structural information from EXAFS

[17],  $^{125}\text{Te}$  Mössbauer spectroscopy [18], and also electronic properties have been earlier investigated [19,20].

In the present paper, particular attention is focused on the compositions  $\text{Ge}_{10}\text{As}_{90-x}\text{Te}_x$  (with  $35 < x < 80$ ) and their preparation. We are interested in the substitution of As for Te in the widest tie line at 10% germanium.

## 2. Experimental procedure

Glassy  $\text{Ge}_{10}\text{As}_{90-x}\text{Te}_x$  ingots (with  $35 < x < 80$ ) were prepared by melt-quenching method. Chemical mixtures of Ge, As and Te (4N purity) were vacuum sealed ( $10^{-5}$  torr) in silica ampoules (3mm id, 4mm od) and slowly heated in a furnace at  $1000^\circ\text{C}$  for 8 hours. The contents of the ampoule were about 1g. The ampoules were agitated continuously during the heating process and during several hours at the melting temperature in order to ensure good homogeneity of the glasses. The experimental set-up is shown in Figure 2. The melt was quenched in iced water at 273K to reach the glassy state of the samples. The quenching rate was estimated to be about 100K/s. Ingots thus obtained were annealed at about  $50^\circ\text{C}$  below the glass transition temperature for 8 hours. The same experimental process was used for compositions of the ternary system.

Characterization and quality of the samples were determined by X-ray diffraction (XRD) and differential scanning calorimetry (DSC). Infrared transmission windows were determined by optical absorption edge ( $E_g$ ) measurements and far infrared transmission spectra (cut-off wavelength,  $\lambda_c$ ).

For XRD experiments, powdered samples were ground manually and placed in a special support. Experiments were carried out on an automated Phillips diffractometer in the bragg-Brentano ( $\theta$ - $2\theta$ ) geometry. The patterns were run with Cu as target using the  $K\alpha$

filtered radiation (Ni filter,  $\lambda = 1.54\text{\AA}$ ) at 40keV and 20mA, and scintillation registration, and were obtained in the range 5-30° in the  $\theta$  scale within multiscan mode. Scanning rate was 0.04°/s, counting rate was 500ms and we used 30 scans.

Glass transition temperature ( $T_g$ ) measurements and thermal behavior were investigated by using a SETARAM DSC 121 differential scanning calorimeter. The temperature calibration was performed using the well known melting temperature of high-purity indium supplied with the instrument. The crystallization thermograms were recorded as the temperature of the samples increased at uniform rate using a dynamic argon atmosphere. Typically, 50mg of sample in powdered form (particle size less than 20 $\mu\text{m}$ ) were sealed in standard quartz tube and scanned over a temperature range from room temperature to about 873K at heating rate  $\alpha = 10\text{K/min}$ . The values of the glass transition temperature ( $T_g$ ), the crystallization peaks ( $T_{c1}$ ,  $T_{c2}$ ) and the melting temperature ( $T_m$ ) were determined with accuracy  $\pm 4\text{K}$  by using the microprocessor of the thermal analyser. Values are reported in **Table 1**. The densities were measured using the Archimedean method along with toluene as a reference medium.

Infrared transmission windows were determined by coupling optical absorption edges measurements (Eg given in **Table 1**) at low wavelengths (UV-visible and near infrared) and infrared transmission at medium and high wavelengths. First, we used a Beckman Acta M IV 5240 equipped with an integration sphere (0.5-3.5eV). Second, the experimental device was a FT-IR BOMEM DA 8 (2.5-50  $\mu\text{m}$ ). Samples were ground, mixed with powdered KBr, the pressed into pallets 13mm diameter and 0.4mm thick. As a example, the transmission window for the  $\text{Ge}_{10}\text{As}_{20}\text{Te}_{70}$  glassy sample is given in Figure 3.

### 3. Results and discussion

#### 3.1. Glass forming ability

Numerous trials were carried out in order to optimize the quenching process (ampoule size, cooling media, melt temperature, batch weight). It was performed for  $\text{Ge}_{20}\text{Te}_{80}$  as can be seen in Figure 4. Trials at  $870^\circ\text{C}$  and  $900^\circ\text{C}$  (melt temperature before quenching) clearly show XRD peaks of the two crystalline c-GeTe and c-Te phases. At  $960^\circ\text{C}$ , broad bumps, typical for the glassy state, appear in the background. Some peaks still presents in the XRD pattern of the sample quenched at  $1000^\circ\text{C}$  in liquid nitrogen. For the same temperature, the melt quenched in iced water give a glassy sample without crystalline phases. This latter procedure was used for ternary compositions. The glassy nature of the synthesized materials has been confirmed by the absence of peaks in XRD patterns of annealed ( $50^\circ\text{C}$  below  $T_g$ ) samples as can be seen in Figure 5. Broad bumps are typical for the glassy state. The position of observed bumps is slightly shifted towards small values of  $\theta$  with the tellurium content.

Variations of the densities of  $\text{Ge}_{10}\text{As}_{90-x}\text{Te}_x$  glassy samples as a function of the ratio  $[\text{Te}]/([\text{Te}] + [\text{As}])$  are represented in **Figure 6**. As can be seen, in the glassy state, densities range from  $5.26$  to  $5.63 \text{ g.cm}^{-3}$ . Values of crystalline c- $\text{As}_2\text{Te}_3$  and c-Te ( $6.23 \text{ g.cm}^{-3}$  and  $6.24 \text{ g.cm}^{-3}$ ), glassy g-  $\text{As}_2\text{Te}_3$  ( $5.65 \text{ g.cm}^{-3}$ ) and g-  $\text{Ge}_{20}\text{Te}_{80}$  ( $5.26 \text{ g.cm}^{-3}$ ), and liquid Te at  $725\text{K}$  ( $5.77 \text{ g.cm}^{-3}$ ) are given for comparison.

### 3.2 Thermal behavior and optical properties

$T_g$  measured by DSC is plotted as function of the ratio  $[\text{Te}]/([\text{Te}] + [\text{As}])$  in Figure 7. For the  $\text{Ge}_{10}\text{As}_{90-x}\text{Te}_x$  samples,  $T_g$  continuously decreases from  $461\text{K}$  ( $x = 36$ ) to  $385\text{K}$  ( $x = 80$ ) with the Te content. After DSC measurements above melting temperature, samples present pronounced changes in the XRD patterns. It is clear that crystallization took place, resulting in the formation of phases which may be identified as Te, As,  $\text{As}_2\text{Te}_3$ ,  $\text{As}_2\text{GeTe}_4$  and  $\text{As}_2\text{Ge}_3\text{Te}_6$  as can be seen in Figure 8. Variation of the absorption edges ( $E_g$ ), represented in Figure 9, is very small due to similar electronic behavior for As and Te. On the contrary, glass

transition temperature variations can be explained because of the substitution of As for Te in terms of connectivity.

### 3.3 Relationship between T<sub>g</sub> and connectivity

For each sample only one value of glass transition temperature (T<sub>g</sub>) was measured by DSC. Decrease of T<sub>g</sub> values with the Te content for Ge<sub>10</sub>As<sub>90-x</sub>Te<sub>x</sub> glasses can be explained by a decrease of the network rigidity. Usual co-ordination numbers (8-N rule) for the Te, As and Ge atoms in chalcogenide glasses are 2, 3 and 4 respectively. The compositional variation of the investigated glasses is characterized by the Te-concentration (x at. %) and/or by the average co-ordination number Z [21,22]. For the Ge<sub>10</sub>As<sub>90-x</sub>Te<sub>x</sub> glasses the average co-ordination number is  $Z = 3.1 - 0.01x$ .

A model commonly used is the Sreeram's model [23,24] based on Gibbs and Di Marzio's work. In this model the authors assume that glasses are formed by chains of twofold co-ordinated atoms (S, Se, or Te in chalcogenide glasses). They make the assumption that T<sub>0</sub> equals to T<sub>g</sub> for the ideal chalcogenide glasses (pure element) where Z equals 2.

Considering thus the average co-ordination number Z, T<sub>g</sub> is ruled by the following law:  $T_g = T_0/[1-\beta(Z-2)]$  where  $\beta$  is characteristic of the system. Hence drawing 1000/T<sub>g</sub> as a function of the crosslinking density (Z-2) gives an estimated value for 1000/T<sub>0</sub>. Values obtained in this work are T<sub>0</sub> = 340±4K and 1/β = 0.40±0.02 for the Ge<sub>10</sub>As<sub>90-x</sub>Te<sub>x</sub> glasses. As a comparison we give here results obtained for binary T<sub>0</sub> = 343K in tellurium, T<sub>0</sub> = 316K in selenium, T<sub>0</sub> = 245K in sulfur based glasses [25,26].

### 3.4 Relationship between T<sub>g</sub> and E<sub>g</sub>

Values reported in

**Tables**



Table 1 and **Table 2** have been used to show (see Figure 10) the correlation between  $T_g$  which reflects the covalency of the chemical bonding between glassy micro domains, and  $E_g$  which is the rigidity of the molecular units composing the micro domains. The linear correlation for the both groups ('Te-rich' and 'As-rich' glasses) clearly show that molecular units are the same and have similar structural behavior. These results are in a good agreement with those previously reported [16, 17].

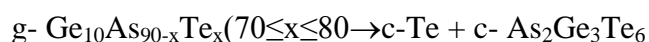
### 3.5 Comparison with the values obtained in the binary system $Sb_2Te_3-As_2Se_3$

The values of the ratio  $[Te]/([Te]+[As])$  of the compositions  $Ge_{10}As_{54}Te_{36}$  (0.400) and  $Ge_{10}As_{50}Te_{40}$  (0.444) of the system Ge-As-Te itself close to those of the compositions  $Sb_{12}As_{28}Se_{42}Te_{18}$  (0.391) and  $Sb_{14}As_{26}Se_{39}Te_{21}$  (0.447) of the  $Sb_2Te_3-As_2Se_3$  system we can thus compare their physical properties ( $\rho$ ,  $E_g$ ,  $T_g$ ,  $T_{c1}$ ,  $T_{c2}$ ,  $T_{c1}-T_g$  and  $T_m$ ) (**Table 2**).

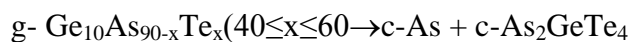
When one replaces germanium by selenium and antimony in the ternary system Ge-As-Te, one notes that the values of the physical properties evolve in the same direction when the ratio  $[Te]/([Te] + [As])$  increase, but they are less low in the system  $Sb_2Te_3-As_2Se_3$ . The aptitude to vitrify glasses of this system (Ge-As-Te) is more important, proving that they are more stable than those of the system  $Sb_2Te_3-As_2Se_3$ .

### 3.6 Crystallization process

In Figure 11, we have represented the thermal behavior (characteristic temperatures) as a function of the ratio  $[Te]/([Te]+ [As])$ . We proposed from XRD patterns and DSC measurements the following crystallization process. In the 'Te-rich' region, crystallization occurs at  $\sim 440K$  for c-Te and at  $\sim 500K$  for  $As_2Ge_3Te_6$ . The crystallization process follows the reaction:



In the ‘As-rich’ region, it occurs above 540K for c-As and  $\text{As}_2\text{GeTe}_4$  and depends on the composition. In this case, the crystallization process is:



For all compositions, melting point occurs in the range [630-650K].

Concerning the thermal stability of the compositions under study, we can see in Figure 11 the ‘As-rich’ glasses present a more stable thermal domain than ‘Te-rich’ glasses. Hence, these compositions are more suitable for drawing glassy fibers devoted to IR sensors technology.

#### 4. Conclusion

We investigated some ternary compositions in the Ge-As-Te system. Particular attention was made in the preparation of the glassy sample. We have optimized the quenching process in order to produce glasses avoiding crystallization. Then, optical properties of these glasses have been studied. Fundamental study of relationships between structure and properties are very important to decide if telluride glasses constitute good candidates for devices involving good optical transmission in the far infrared domain. We also studied their thermal stability in order to choose a glass presenting optimal performance for drawing fibers without crystalline domains. A comparison of the properties of glasses of the ternary system Ge-As-Te was done with those of glasses of the binary system  $\text{Sb}_2\text{Te}_3\text{-As}_2\text{Se}_3$ . It made it possible to show that the substitution of germanium by selenium and antimony reduces the physical properties ( $\rho$ ,  $E_g$ ,  $T_g$ ,  $T_{c1}$ ,  $T_{c2}$ ,  $T_{c1}-T_g$  et  $T_m$ ). Indeed germanium supports the formation of glasses, contrary to metal antimony.

## Tables

**Table 1.** The ratio  $[\text{Te}]/([\text{Te}] + [\text{As}])$  is taken in order to compare  $\text{Ge}_{10}\text{As}_{90-x}\text{Te}_x$  and  $\text{Ge}_{20}\text{Te}_{80}$  glasses. This ratio increases when Te content  $x$  increases. Densities are given in  $\text{g}\cdot\text{cm}^{-3}$ . Optical absorption edges ( $E_g$ ) are given in eV. Glass transition temperature ( $T_g$ ), first ( $T_{c1}$ ) and eventually second ( $T_{c2}$ ) crystallization temperature, and melting temperature of glassy compositions are given in K (error bars  $\pm 4\text{K}$ ).

Composition	$[\text{Te}]/([\text{Te}] + [\text{As}])$	Density ( $\pm 0.18$ )	$E_g$ ( $\pm 0.03$ )	$T_g$	$T_{c1}$	$T_{c2}$	$T_{c1} - T_g$	$T_m$
$\text{Ge}_{10}\text{As}_{54}\text{Te}_{36}$	0.400	5.26	-	461	580	-	119	639
$\text{Ge}_{10}\text{As}_{50}\text{Te}_{40}$	0.444	5.54	0.92	449	549	571	100	649
$\text{Ge}_{10}\text{As}_{46}\text{Te}_{44}$	0.488	5.34	0.89	439	539	550	100	651
$\text{Ge}_{10}\text{As}_{20}\text{Te}_{70}$	0.777	5.63	0.83	403	442	497	39	628
$\text{Ge}_{10}\text{As}_{16}\text{Te}_{74}$	0.822	5.32	0.81	397	433	506	36	648
$\text{Ge}_{10}\text{As}_{10}\text{Te}_{80}$	0.888	-	0.79	385	449	504	64	645
$\text{Ge}_{20}\text{Te}_{80}$	1.000	5.26	0.72	420	443	503	23	640

**Table 2.** Comparison of the values of the physical properties ( $\rho$ ,  $E_g$ ,  $T_g$ ,  $T_{c1}$ ,  $T_{c2}$ ,  $T_{c1} - T_g$  and  $T_m$ ) of two compositions of the ternary system Ge-As-Te those their counterparts of the  $\text{Sb}_2\text{Te}_3\text{-As}_2\text{Se}_3$  binary system.

Compositions	$[\text{Te}]/([\text{Te}] + [\text{As}])$	Density ( $\pm 0.18$ )	$E_g$ ( $\pm 0.03$ )	$T_g$	$T_{c1}$	$T_{c2}$	$T_{c1} - T_g$	$T_m$
$\text{Ge}_{10}\text{As}_{54}\text{Te}_{36}$	0.400	5.26	-	461	580	-	119	639
(A) $\text{Sb}_{12}\text{As}_{28}\text{Se}_{42}\text{Te}_{18}$	0.391	5.16	0.85	426	478	525	52	607
$\text{Ge}_{10}\text{As}_{50}\text{Te}_{40}$	0.444	5.54	0.92	449	549	571	100	649
(B) $\text{Sb}_{14}\text{As}_{26}\text{Se}_{39}\text{Te}_{21}$	0.447	---	---	422	456	517	34	580

### Figure captions

**Figure 1.** Glass forming regions in the ternary Ge-As-Te: ( $\blacktriangle$ ) crystalline phases. For pseudo-binary  $\text{As}_2\text{Te}_3\text{-nGeTe}$ , n values are represented (n = 1, 3 and 5). Chemical compositions of prepared glasses ( $\bullet$ ) and partially crystallized samples ( $\circ$ ) are represented

**Figure 2.** Experimental set-up used for glass preparation. Vibrator was used to avoid/remove bubbles in glassy samples. The trap door was opened only during the quenching process into the cooling media (here iced water).

**Figure 3.** Transmission window of  $\text{Ge}_{10}\text{As}_{20}\text{Te}_{70}$  glassy sample. Low wavelengths spectrum was obtained from optical absorption edge measurements.

**Figure 4.** X-Ray diffraction patterns of as-quenched samples as a function of the melting temperature and the cooling media for the  $\text{Ge}_{20}\text{Te}_{80}$  composition. Observed diffraction peaks were attributed to the c-Te ( $\blacksquare$ ) and c-GeTe ( $\circ$ ) crystalline phases.

**Figure 5.** X-ray diffraction patterns of glassy samples under investigation. No diffraction peak was observed in these glasses.

**Figure 6.** Evolution of the density as a function of the ratio  $[\text{Te}]/([\text{Te}]+[\text{As}])$ . Glassy g- $\text{As}_2\text{Te}_3$  and g- $\text{Ge}_{20}\text{Te}_{80}$ , crystalline c-  $\text{As}_2\text{Te}_3$  and c-Te and liquid Te at 725K are drawn for comparison. Open circles ( $\circ$ ) correspond to ‘Te-rich’ glasses. Solid squares ( $\blacksquare$ ) correspond to ‘As-rich’ glasses. The star labeled A corresponds to  $\text{Sb}_{12}\text{As}_{28}\text{Se}_{42}\text{Te}_{18}$  glassy composition.

**Figure 7.** Evolution of the glass transition temperature ( $T_g$ ) as a function of the ratio  $[\text{Te}]/([\text{Te}]+[\text{As}])$ . Open circles ( $\circ$ ) correspond to ‘Te-rich’ glasses. Solid squares ( $\blacksquare$ ) correspond to ‘As-rich’ glasses. Stars labeled A and B correspond to  $\text{Sb}_{12}\text{As}_{28}\text{Se}_{42}\text{Te}_{18}$  and  $\text{Sb}_{14}\text{As}_{26}\text{Se}_{39}\text{Te}_{21}$  glassy compositions respectively.

**Figure 8.** X-ray diffraction patterns of annealed samples after DSC measurements. Different crystalline phases have been attributed: c-Te and  $\text{As}_2\text{Ge}_3\text{Te}_6$  in the ‘Te-rich’ region, and As and  $\text{As}_2\text{GeTe}_4$  in the ‘As-rich’ region.

**Figure 9.** Evolution of the optical absorption edge ( $E_g$ ) as a function of the ratio  $[\text{Te}]/([\text{Te}]+[\text{As}])$ . Open circles ( $\circ$ ) correspond to ‘Te-rich’ glasses. Solid squares ( $\blacksquare$ ) correspond to ‘As-rich’ glasses. The star labeled A corresponds to  $\text{Sb}_{12}\text{As}_{28}\text{Se}_{42}\text{Te}_{18}$  glassy composition.

**Figure 10.** Correlation between optical gap ( $E_g$ ) and glass transition temperatures ( $T_g$ ) for compositions described in this study. Open circles ( $\circ$ ) correspond to ‘Te-rich’ glasses. Solid squares ( $\blacksquare$ ) correspond to ‘As-rich’ glasses. The star labeled A corresponds to  $\text{Sb}_{12}\text{As}_{28}\text{Se}_{42}\text{Te}_{18}$  glassy composition.

**Figure 11.** Representation of the thermal behaviour of the glassy samples. Glass transition temperatures (■□), crystallisation temperature (▲▼Δ▽) and melting point (●) are drawn as a function of the ratio  $[Te]/([Te]+[As])$ . Solid lines are drawn in order to give an idea of the thermal stability of the glassy compositions and represent  $(T_c - T_g)$  quantity. (see text for details)

## References

- <sup>1</sup> C.H. Seager, D. Emin, R.K. Quinn, *Phys. Rev.*, **B8** (1973) 4746.
- <sup>2</sup> H. Krebs, P. Fischer, *Discuss. Farad.*, **50** (1970) 35.
- <sup>3</sup> J.A. Savage, S. Nielsen, *Infrared Physics*, **5** (1965) 195.
- <sup>4</sup> A.B. Seddon, *J. Non Cryst. Solids*, **184** (1995) 44.
- <sup>5</sup> S.S.K. Titus, S. Asokan, T.S. Panchapagesan, E.S.R. Gopal, *Phys. Rev.*, **B46** (1992) 14493.
- <sup>6</sup> S. Asokan, E.S.R. Gopal, *Rev. Solid State Sci.*, **3** (1989) 273.
- <sup>7</sup> J.A. Savage, S. Nielsen, *Phys. Chem. Glasses*, **7** (1966) 56.
- <sup>8</sup> P.P. Seregin, V.P. Sivkov, F.S. Nasredinov, L.N. Vasilev, Yu V. Krylnikov and Yu P. Kostinov, *Phys. Stat. Sol.*, (a) **39** (1977) 437.
- <sup>9</sup> B. Bureau, S. Danto, H. Li Ma, C. Boussard-Plédel, X. H. Zhang, J. Lucas, *Solid State Sciences* **10** (2008) 427.
- <sup>10</sup> J. Cornet, D. Rossier, *J. Non Cryst. Solids*, **12** (1973) 61.
- <sup>11</sup> D.J. Sarach, J.P. de Neufville, W.L. Haworth, *J. Non Cryst. Solids*, **22** (1976) 245.
- <sup>12</sup> H.W. Shu, S. Jaulmes, J. Flahaut, *J. Solid State Chem.*, **74** (1988) 277.
- <sup>13</sup> R. Ollitrault-Fichet, H.W. Shu, J. Rivet, J. Flahaut, *Mat. Res. Bull.* **24** (1989) 351.
- <sup>14</sup> A.R. Hilton, C.E. Jones, M. Brau, *Infrared Phys.*, **6** (1966) 183.
- <sup>15</sup> J.A. Savage, *J. Non Cryst. Solids*, **11** (1972) 121.
- <sup>16</sup> J.A. Savage, *J. Mater. Sci.*, **6** (1971) 964.
- <sup>17</sup> P.E. Lippens, J.C. Jumas, J. Olivier-Fourcade, L. Aldon, *J. Non Cryst. Solids*, **271** (2000) 119.
- <sup>18</sup> L. Aldon, P.E. Lippens, J.C. Jumas, J. Olivier-Fourcade, H. Bemelmans, G. Langouche, *J. Non Cryst. Solids*, **262** (2000) 244.
- <sup>19</sup> P.E. Lippens, J.C. Jumas, J. Olivier-Fourcade, L. Aldon, *J. Phys. Chem. Solids*, **61** (2000) 1761.
- <sup>20</sup> L. Aldon, *Ph. D thesis* (December 1996), Université Montpellier II, France.
- <sup>21</sup> K. Tanaka, *Phys. Rev.*, **B39** (1989) 1270.
- <sup>22</sup> J.P. de Neufville, H.K. Rockstad, *Proc. Amorphous Solids and Liquid semiconductors*, (1974) 449.
- <sup>23</sup> A.N. Sreeram, D.R. Swiler, A.J.K. Varshneya, *J. Non Cryst. Solids*, **127** (1991) 287.
- <sup>24</sup> A.J.K. Varshneya, A.N. Sreeram, D.R. Swiler, *Phys. Chem. Glasses*, **34** (1993) 179.
- <sup>25</sup> R. Kerner, M. Micoulaut, *J. Non Cryst. Solids*, **210** (1997) 298.
- <sup>26</sup> M. Micoulaut, *Eur. Phys. J.*, **B1** (1998) 277.